

Generation of isolated attosecond pulses with a specific waveform two-color laser field

Jinping Yao (姚金平)^{1,2*}, Yao Li (李 耀)^{1,2}, and Ya Cheng (程 亚)¹

¹State Key Laboratory of High Field Laser Physics, Shanghai Institute of Optics and Fine Mechanics, Chinese Academy of Sciences, Shanghai 201800, China

²Graduate University of the Chinese Academy of Sciences, Beijing 100049, China

*Corresponding author: jinpingsmrg@163.com

Received November 2, 2010; accepted November 26, 2010; posted online March 14, 2011

We theoretically propose a new method for generating intense isolated attosecond pulses during high-order harmonic generation (HHG) process by accurately controlling electron motion with a two-color laser field, which consists of an 800-nm, 4-fs elliptically polarized laser field and a 1400-nm, ~ 43 -fs linearly polarized laser field. With this method, the supercontinua with a spectral width above 200 eV are obtained, which can support a ~ 15 -as isolated pulse after phase compensation. Classical and quantum analyses explain the controlling effects well. In particular, when the pulse duration of the 800-nm laser field increases to 20-fs, sub-100-as isolated pulses can be obtained even without any phase compensation.

OCIS codes: 190.4160, 340.7480, 020.2649.

doi: 10.3788/COL201109.041901.

The birth of attosecond (10^{-18} s) extreme ultraviolet (XUV) pulses has opened the door to an investigation on dynamic evolutions of electron states with unprecedented time resolution^[1]. In the last several years, a series of methods has been explored to generate isolated attosecond pulses (IAPs) during the high-order harmonic generation (HHG) process^[2]. The first method is to utilize few-cycle driving pulses^[3,4]. Using this straightforward way, an isolated ~ 80 -as pulse has been generated by a 3.3-fs, carrier-envelope phase (CEP) stabilized laser field^[4]. However, only very few laboratories can produce such short driving pulses. The second method is polarization gating technology^[5]. Although this technique has been experimentally demonstrated, it still requires the state-of-the-art 5-fs pump pulses and cannot generate intense IAPs. Recently, the two-color field scheme has been intensively investigated both theoretically and experimentally^[6-12]. With this method, both an extremely broadened XUV supercontinuum and a significantly extended cutoff energy are obtained that allow us to create IAPs with multi-cycle laser pulses. In addition to the abovementioned methods, some combined methods have been proposed, such as double optical gating^[13], generalized double optical gating^[14], utilizing orthogonal-polarized two-color laser field^[15,16], utilizing neither orthogonal-polarized nor parallel-polarized two-color laser field^[17], and so on.

In this letter, we demonstrate an alternative method to obtain intense IAPs with a laser field composed of an 800-nm, 4-fs elliptically polarized laser field and a 1400-nm, ~ 43 -fs linearly polarized field. The synthesized field can accurately manipulate electron motion and effectively select short quantum trajectories. The physical mechanism behind the controlling effect is explored. Lastly, we propose that this method is still feasible in a multi-cycle regime.

In our calculation, the driving field consists of an 800-nm, 4-fs elliptically polarized laser field and a 1400-nm, ~ 43 -fs linearly polarized laser field, which can be

expressed as

$$E_x = E_1 \exp[-2 \ln(2) \cdot t^2 / \tau_1^2] \sin(\omega_1 t) / \sqrt{1 + \varepsilon^2}, \quad (1)$$

$$E_y = E_1 \exp[-2 \ln(2) \cdot t^2 / \tau_1^2] \cos(\omega_1 t) \cdot \varepsilon / \sqrt{1 + \varepsilon^2} + \sqrt{A} \cdot E_1 \exp[-2 \ln(2) \cdot (t + T_d)^2 / \tau_2^2] \sin[\omega_2(t + T_d)], \quad (2)$$

where E_1 is the amplitude of the 800-nm laser field; and A and T_d are the intensity ratio and time delay between the 800 and 1400-nm pulses, respectively; ω_i , τ_i ($i=1, 2$)

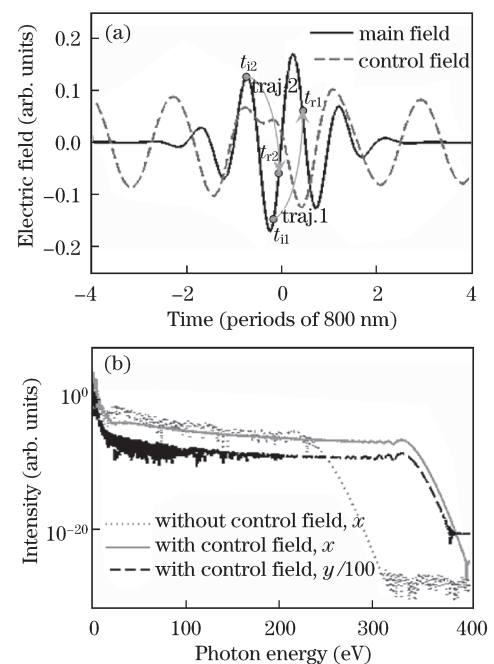


Fig. 1. (a) Electric fields of the main field and the control field; (b) HH spectrum generated with the main field alone and spectra of HHs emitted along the x and y directions when the control field is introduced.

denote angular frequency and pulse duration of 800- ($i=1$) and 1400-nm laser field ($i=2$), respectively. The peak intensity of the 800-nm pulse was fixed at 1.2×10^{15} W/cm², and its ellipticity ε was set as 0.3. The intensity ratio A is limited in the range of 0.02–0.33. Given that the x -component of the synthesized field is much stronger than its y -component, we call the x - and y -components of the synthesized field as “main field” and “control field”, respectively.

From the Lewenstein model^[18] of HHG, we know that the dominant contribution to the harmonic emission comes from the electron, which tunnels away from the nucleus but reencounters it after accelerating in the laser field. This means that when the electron returns, its displacement from its parent ion is zero.

$$\begin{cases} x_s = x_{800}(t_i, t_r) = 0 \\ y_s = y_{800}(t_i, t_r) + y_{1400}(t_i, t_r, A, T_d) = 0. \end{cases} \quad (3)$$

In principle, by adjusting the parameters A and T_d , one can make the electron born at the time t_i return at the time t_r (i.e., $x_s = 0$, $y_s = 0$) and make the electron born at other time far from its parent ion (i.e., $x_s = 0$, $y_s \gg 0$). In this way, we can create HHG mainly from the recollision of electrons ionized within a certain amount of time, beyond which HHG can be effectively suppressed or weakened due to the large displacement of the electron from its parent ion. Naturally, the number of electron recollision is effectively reduced, which makes it possible to generate an isolated XUV pulse. In order to confirm our idea, the single-atom response of HHG was calculated with the Lewenstein model^[18]. The atom gas used in the calculations was helium (He). The harmonic spectrum was obtained by Fourier transforming the time-dependent dipole moment.

First, we solved Eq. (3) under the conditions of $t_i = t_{i1}$ and $t_r = t_{r1}$. With the main field alone, the electron born at the time t_{i1} definitely returned at the time t_{r1} (i.e., $x_s = 0$) and obtained maximum kinetic energy. There is a series of A and T_d to satisfy the equation $y_s = 0$, among which an extremely broad and smooth XUV supercontinuum is achieved when $A \approx 0.23$ and $T_d \approx 2.63$ fs. The corresponding electric fields are shown in Fig. 1(a). As can be seen, the main field is a sine-waveform field, while the control field varies from one half-cycle to the next one. For comparison, Fig. 1(b) shows high-order harmonic (HH) spectra generated with the main field alone and with the synthesized field composed of the main field and the control field. In the case without the control field, some modulation appears in the cutoff region of the harmonic spectrum, which is due to the interference between high-order harmonics (HHs) from the trajectory 1 (t_{i1}, t_{r1}) and the trajectory 2 (t_{i2}, t_{r2}), as shown in Fig. 1(a). When the control field determined by the optimized A and T_d is superposed onto the main field, the XUV supercontinuum is dramatically broadened, and the cutoff energy of HHs is extended to ~ 330 eV. Here, the spectral intensity of HHs emitted along the y direction is purposely reduced by 2 orders of magnitude for display purposes only. When the control field is introduced, the spectrum of HHs emitted along the x direction exhibits an extremely smooth supercontinuum, which covers the entire plateau region; meanwhile, the

spectrum of HHs emitted along the y direction shows small modulation at the beginning of the plateau region. In addition, HHs generated with the control field have nearly the same intensity as HHs generated without the control field.

In Fig. 2, we show attosecond pulses obtained by inverse Fourier transforming the XUV supercontinuum within the spectral range of 100–330 eV, which is generated by the synthesized field. Figure 2(a) presents the electric fields of attosecond pulses in a three-dimensional (3D) space. The x -component of the electric field corresponds to a well IAP. However, in the y direction, a main attosecond pulse is accompanied by a satellite pulse. Figure 2(b) shows the envelopes of attosecond pulses that are defined as the summation of the intensities of attosecond pulses emitted along x and y directions. Due to the fact that the satellite pulse is ~ 2 orders of magnitude weaker than the main attosecond pulse, the main attosecond pulse can be regarded as a well IAP with the pulse duration of ~ 92 as. After phase compensation, its pulse duration is reduced to ~ 15 as, which is shorter than an atomic unit (a. u.).

In order to explore physical mechanisms underlying the broadening of the XUV supercontinua, we perform theoretical analyses as follows. Figures 3(a) and (b) show the time-frequency analyses of the x -component of the dipole moment in the cases without and with the control field, respectively. The corresponding classical analyses based on the three-step model of HHG^[19] are shown in Figs. 3(c) and (d). As shown in Fig. 3(a), in the case without the control field, the electrons following trajectory 1 (t_{i1}, t_{r1}) and trajectory 2 (t_{i2}, t_{r2}) have nearly equal return

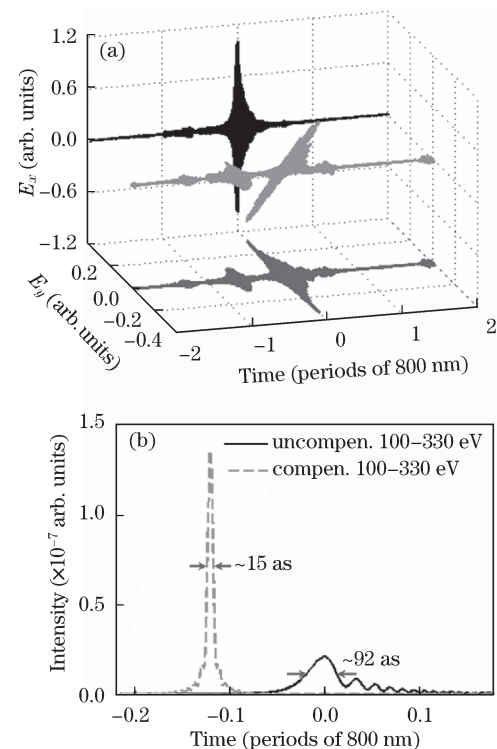


Fig. 2. (a) 3D electric fields and (b) intensity envelopes of attosecond pulses obtained by inverse Fourier transforming the supercontinua generated with the synthesized field in Fig. 1(a).

energy, and on the two sides of trajectory 1, there are two arms with comparable intensity, which correspond to long trajectories and short trajectories, respectively^[20]. The classical analysis in Fig. 3(c) is in good agreement with the quantum analysis in Fig. 3(a). Clearly, the electrons born at the time t_{i1} and t_{i2} both achieve return kinetic energy E_k of ~ 200 eV (dashed line); however, the electron born around the time t_{i1} has much higher ionization rate (filled curve) than the electron born around the time t_{i2} . When the control field is superposed onto the main field, the electron following the trajectory 1 (t_{i1}, t_{r1}) obtains higher return kinetic energy, while the electron following the trajectory 2 (t_{i2}, t_{r2}) no longer emits HHs [Fig. 3(b)]. In addition, the long trajectory near the trajectory 1 disappears after the use of the control field. In the Fig. 3(d), we also investigate the displacement of the electron from its parent ion Δr ($\Delta r = \sqrt{x_s^2 + y_s^2}$) (solid line) as a function of the birth time of electron. The displacement is defined as the closest distance between the electron and its parent ion within an optical period of 1400 nm after ionization. The electron born at the time t_{i1} exactly returns to its parent ion (i.e., $\Delta r = 0$) at the time t_{r1} . Nevertheless, the electron born at the time t_{i2} has a displacement ~ 130 a. u. from its parent ion, which is so large that the electron cannot recombine with its parent ion. Therefore, the harmonic emission from trajectory 2 is suppressed. Moreover, when the electron is born slightly before the time t_{i1} , Δr rapidly increases with the birth time; in contrast, when the electron is born slightly after it, Δr changes slowly, resulting in the natural selection of a short trajectory. For the selected trajectory, due to the high ionization rate and small displacement of the electron from its parent ion, the XUV supercontinua are sufficiently intense.

Finally, it is worth pointing out that this method is still feasible even in a multi-cycle regime. When pulse duration of the 800-nm laser field increases to 20 fs, with other parameters unchanged, the XUV supercontinuum emitted along the x direction is still extremely broad and smooth, covering a photon energy range of 250–350 eV [Fig. 4(a)]. The supercontinuum emitted along the y

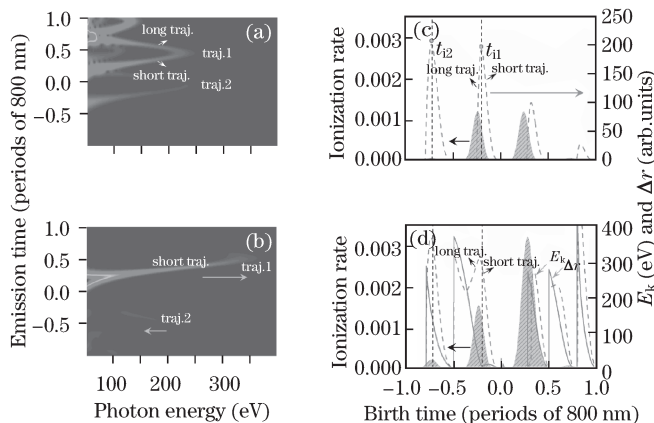


Fig. 3. Time-frequency analyses of the x -component of dipole moment in the case (a) without the control field and (b) with the control field. The return kinetic energy of electron E_k (dashed line), the ionization rate (filled curve), and the electron displacement from its parent ion Δr (solid line) as a function of the birth time of electron in the case (c) without the control field and (d) with the control field.

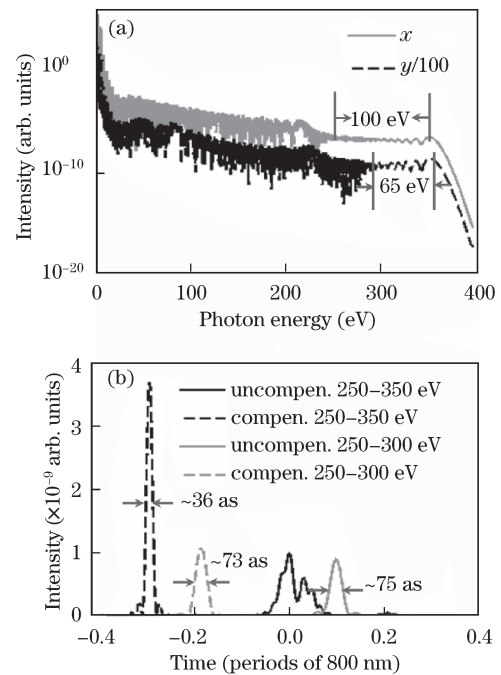


Fig. 4. (a) Spectra of HHs emitted along the x and y directions and (b) intensity envelopes of attosecond pulses synthesized from the HH spectra in Fig. 4(a) when the pulse duration of 800-nm laser field increases to 20 fs. Curves in Fig. 4(b) are temporally shifted for clarity.

direction has a spectral width of 65 eV and shows a relatively deep modulation. Therefore, attosecond pulses synthesized by HHs in the spectral range show a multiple-peak structure [Fig. 4(b)]. After phase compensation, the supercontinua can support the ~ 36 -as pulse. Meanwhile, an isolated ~ 75 -as pulse is created when the harmonic spectrum within the range of 250–300 eV is selected, and this pulse is close to Fourier-transform-limited (e.g., ~ 73 as).

In conclusion, we propose a new and easily performed method to generate IAPs. When a 1400-nm, ~ 43 -fs linearly polarized field is superimposed in the minor-axis direction of an 800-nm, 4-fs elliptically field, not only an effectively extended cutoff energy but also an ultrabroad XUV supercontinuum is observed. The supercontinuum with a spectral range of 100–330 eV can support an isolated ~ 15 -as pulse after phase compensation. Theoretical analyses demonstrate that with the synthesized field, the number of electron trajectories contributing to HHG is effectively reduced, and short quantum trajectory is well selected, thereby dominating the broadening of the XUV supercontinuum. In particular, this method is still feasible in the multi-cycle regime, which largely reduces the requirement for pulse duration of pump pulses and makes it possible to generate intense IAPs in the future.

This work was supported by the National Natural Science Foundation of China under Grant No. 60921004.

References

1. P. Agostini and L. F. DiMauro, Rep. Prog. Phys. **67**, 813 (2004).
2. F. Krausz and M. Ivanov, Rev. Mod. Phys. **81**, 163 (2009).

3. J. J. Carrera, X. M. Tong, and S.-I. Chu, *Phys. Rev. A* **74**, 023404 (2006).
4. E. Goulielmakis, M. Schultze, M. Hofstetter, V. S. Yakovlev, J. Gagnon, M. Uiberacker, A. L. Aquila, E. M. Gullikson, D. T. Attwood, R. Kienberger, F. Krausz, and U. Kleineberg, *Science* **320**, 1614 (2008).
5. G. Sansone, E. Benedetti, F. Calegari, C. Vozzi, L. Avaldi, R. Flammini, L. Poletto, P. Villoresi, C. Altucci, R. Velotta, S. Stagira, S. De Silvestri, and M. Nisoli, *Science* **314**, 443 (2006).
6. T. Pfeifer, L. Gallmann, M. J. Abel, D. M. Neumark, and S. R. Leone, *Opt. Lett.* **31**, 975 (2006).
7. Z. Zeng, Y. Cheng, X. Song, R. Li, and Z. Xu, *Phys. Rev. Lett.* **98**, 203901 (2007).
8. C. Vozzi, F. Calegari, F. Frassetto, L. Poletto, G. Sansone, P. Villoresi, M. Nisoli, S. D. Silvestri, and S. Stagira, *Phys. Rev. A* **79**, 033842 (2009).
9. P. Lan, P. Lu, W. Cao, Y. Li, and X. Wang, *Phys. Rev. A* **76**, 011402(R) (2007).
10. B. Zeng, Y. Yu, W. Chu, J. Yao, Y. Fu, H. Xiong, H. Xu, Y. Cheng, and Z. Xu, *J. Phys. B* **42**, 145604 (2009).
11. G. Chen, J. Chen, and Y. Yang, *Acta Opt. Sin.* (in Chinese) **29**, 3255 (2009).
12. X. Du, X. Zhou, and P. Li, *Chinese J. Lasers* (in Chinese) **37**, 1213 (2010).
13. H. Mashiko, S. Gilbertson, C. Li, S. Khan, M. M. Shakya, E. Moon, and Z. Chang, *Phys. Rev. Lett.* **100**, 103906 (2008).
14. X. Feng, S. Gilbertson, H. Mashiko, H. Wang, S. D. Khan, M. Chini, Y. Wu, K. Zhao, and Z. Chang, *Phys. Rev. Lett.* **103**, 183901 (2009).
15. Y. Yu, X. Song, Y. Fu, R. Li, Y. Cheng, and Z. Xu, *Opt. Express* **16**, 686 (2008).
16. Y. Yu, J. Xu, Y. Fu, H. Xiong, H. Xu, J. Yao, B. Zeng, W. Chu, J. Chen, Y. Cheng, and Z. Xu, *Phys. Rev. A* **80**, 053423 (2009).
17. J. Yao, Y. Li, B. Zeng, H. Xiong, H. Xu, Y. Fu, W. Chu, J. Ni, X. Liu, J. Chen, Y. Cheng, and Z. Xu, *Phys. Rev. A* **82**, 023826 (2010).
18. M. Lewenstein, P. Balcou, M. Y. Ivanov, A. L'Huillier, and P. B. Corkum, *Phys. Rev. A* **49**, 2117 (1994).
19. P. B. Corkum, *Phys. Rev. Lett.* **71**, 1994 (1993).
20. A. Scrinzi, M. Y. Ivanov, R. Kienberger, and D. M. Villeneuve, *J. Phys. B: At. Mol. Opt. Phys.* **39**, R1 (2006).